Boron nitride nanotubes functionalized with mesoporous silica for intracellular delivery of chemotherapy drugs

ARTICLE *in* CHEMICAL COMMUNICATIONS · JULY 2013

Impact Factor: 6.83 · DOI: 10.1039/c3cc42743a · Source: PubMed

6 AUTHORS, INCLUDING:

Xia Li
National Institute for Materials Science
45 PUBLICATIONS **767** CITATIONS
SEE PROFILE

Dmitri Golberg
National Institute for Materials Science
639 PUBLICATIONS **21,950** CITATIONS
SEE PROFILE

ChemComm

RSC Publishing

COMMUNICATION

View Article Online
View Journal | View Issue

Cite this: *Chem. Commun.*, 2013, **49**, 7337

Received 18th April 2013,
Accepted 18th June 2013

DOI: 10.1039/c3cc42743a

www.rsc.org/chemcomm

Boron nitride nanotubes functionalized with mesoporous silica for intracellular delivery of chemotherapy drugs†

Xia Li,*[a] Chunyi Zhi,[b] Nobutaka Hanagata,*[c] Maho Yamaguchi,[a] Yoshio Bando[a] and Dmitri Golberg*[a]

Boron nitride nanotube (BNNT)@mesoporous silica hybrids with controllable surface zeta potential were fabricated for intracellular delivery of doxorubicin. The materials showed higher suspension ability, doxorubicin intracellular endocytosis efficiency, and LNcap prostate cancer cell killing ability compared with naked BNNTs.

Boron nitride nanotubes (BNNTs), as structural analogues of carbon nanotubes (CNTs), have recently attracted a lot of attention in the biomedical field, *e.g.* with respect to bone tissue engineering,[1] drug delivery,[2] boron neutron capture cancer therapy,[3] irreversible lethal electroporation cancer treatment,[4] *etc.* Overall, multi-walled BNNTs show better biocompatibility than CNTs,[1,5] although too long BNNTs result in structural cytotoxicity.[6] The exploration of BNNTs for cancer therapy is a promising direction. BNNTs[3] and CNTs with C_2B_{10} carborane cages attached[7] have shown higher concentration of boron atoms in tumour cells than in blood and other organs, which makes them attractive nanovehicles for the delivery of B to tumour cells for effective B neutron capture for cancer therapy and diagnostics. On the other hand, the exploration of BNNTs as an anti-cancer drug delivery system could provide an integrated vector system by combining chemotherapy with radiation therapy or electroporation cancer therapy. Up to now, little has been done to devise rational strategies for binding anti-cancer drug molecules onto BNNTs, although theoretical calculations have shown that BNNTs are more ideal delivery capsules, compared with other nanotubes, such as carbon, silicon and boron carbide nanotubes.[8]

It is known that the sidewalls of pristine BNNTs are highly hydrophobic and are easily aggregated. The BNNT functionalization for aqueous solubility is necessary. Although some organic molecules, such as polymers[9] and peptides,[10] have been used to improve the stability of BNNT suspensions, the organic molecules are easily degraded or detached due to the presence of some enzymes *in vivo*. Oxidation and shortening of BNNTs improved the suspension ability and DNA loading to only a certain extent,[11] which is still not satisfactory. The functionalization of BNNTs with silica, a well-proved material with excellent biocompatibility and abundant surface groups, to fabricate core–shell structure,[12] gives the opportunity to improve the suspension ability and hydrophilicity, to control the surface charge and thus to manipulate the intracellular drug delivery.

Herein, we confirm that functionalization of BNNTs with mesoporous silica (i) improved their aqueous suspension ability; (ii) helped to easily control the surface zeta potential; and (iii) enabled binding of drug molecules to functionalized BNNTs, increasing the endocytosis efficiency of doxorubicin (dox) 3–4 times. The designed pathways may not only be effective for isolating BNNTs in aqueous media but may also promote fabrication of functionalized BNNTs and expansion of their future biomedical applications, especially in cancer therapy.

BNNT@mesoporous silica composites with a negative charge (BNNT@mesoporous silica composites, BNNT@MS) and a positive charge (BNNT@mesoporous silica composites grafted with the amino group, BNNT@MS–NH_2) were fabricated. As illustrated in Scheme 1, the strategy to form mesoporous silica on the outer surface of BNNTs is as follows: the cationic surfactant, cetyltrimethyl ammonium bromide (CTAB), interacted strongly with BNNTs in solution *via* van der Waals forces and was adsorbed onto their outer surfaces.[13] This resulted in the formation of stable BNNT–CTAB surfactant supermolecular structure and gave a high local concentration of CTAB on the surface of BNNTs compared to the bulk solution. After tetraethyl orthosilicate (TEOS) or a mixture of TEOS and 3-aminopropyltrimethoxysilane (APTMS) was added into the above solution, it hydrolyzed and condensed into silicate polyanions, which cooperatively self-assembled with positively charged groups of cationic surfactant CTAB on the BNNT surfaces. The obtained product was washed several times by centrifugation and redispersion in ethanol to remove the template.

The as-prepared BNNTs synthesized by chemical vapour deposition (CVD)[14] were oxidized in air at 1000 °C for 5 h and

[a] *World Premier International Center for Materials Nanoarchitectonics (WPI-MANA), National Institute for Materials Science (NIMS), Namiki 1-1, Tsukuba, Ibaraki 305-0044, Japan. E-mail: GOLBERG.Dmitri@nims.go.jp, LI.Xia@nims.go.jp*
[b] *Department of Physics and Materials Science, City University of Hong Kong, Tat Chee Avenue, Kowloon, Hong Kong*
[c] *Nanotechnology Innovation Station, National Institute for Materials Science (NIMS), 1-2-1 Sengen, Tsukuba, 305-0047, Japan. E-mail: HANAGATA.Nobutaka@nims.go.jp*

† Electronic supplementary information (ESI) available. See DOI: 10.1039/c3cc42743a

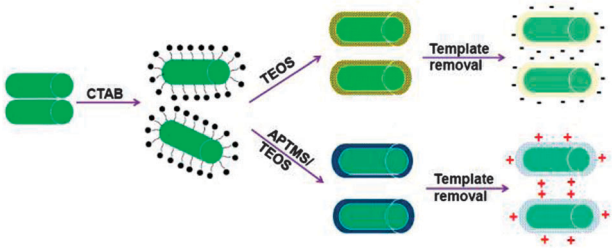

Scheme 1 Formation process of BNNT@mesoporous silica.

sonicated in water to obtain the shortened BNNTs, around 1 μm long (Fig. S1, ESI†). Synthesis of BNNT@MS was carried out by the hydrolysis of TEOS in the presence of CTAB. By fixing the ratio of CTAB/BN/H_2O and changing the amount of TEOS, the shell thickness of mesoporous silica was adjusted from 5 nm to 20 nm, as revealed by TEM (Fig. 1). By changing the silica source to the mixture of TEOS and 3-aminopropyltrimethoxysilane (APTMS), the positively charged BNNT@MS–NH_2 hybrids grafted with amino groups were obtained. The obtained products were dispersed in water for more than 24 h and dispersed again by slight shaking when sedimentation had occurred. Whereas the naked BNNTs could be dispersed in water only for 3 h after strong sonication treatment. And once sedimentation had occurred for BNNTs, the dispersion status was difficult to recover by shaking. Thus, it can be concluded that the mesoporous silica shell enhanced the suspension ability and hydrophilic properties of BNNTs in an aqueous solution. In addition, the oxidation treatment of the as-prepared BNNTs in air was important for the subsequent formation of mesoporous silica on the BNNT surface. When H_2O_2 oxidation treated BNNTs were used as precursors, the mesoporous silica shell could not uniformly form on their surface (Fig. S2, ESI†). The N_2 adsorption–desorption isotherms (Fig. S3, ESI†) exhibited the type IV isotherm curves with a step between 0.4 and 0.9 P/P_0 for BNNT@MS and BNNT@MS–NH_2, which indicates the presence of mesoporous structure. Both hybrids showed the increased specific surface area of 799 and 465 $m^2\ g^{-1}$, respectively, compared with that of pristine BNNTs of about 131 $m^2\ g^{-1}$. The pore sizes of both BNNT@MS and BNNT@MS–NH_2 were centred at approximately 1.8 nm.

The surface functionalization of BNNTs after their modification with mesoporous silica was analyzed using the zeta potential measurements and Fourier transform infrared (FTIR) spectroscopy. In contrast to the zeta potential of −5 mV for BNNTs, the values of zeta potential for BNNT@MS and BNNT@MS–NH_2 became negative, around −15 mV, and positive, around 6 mV, respectively (Fig. 2A).

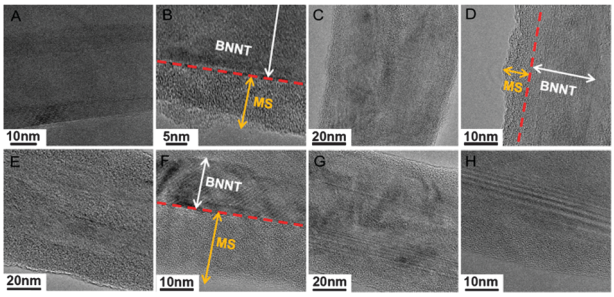

Fig. 1 TEM images of BNNT (A), BNNT@MS (B), BNNT@MS(−) (C and D), BNNT@MS(+) (E and F) and BNNT@MS–NH_2 (G and H) samples.

FTIR spectroscopy measurements were carried out to comparatively analyze BNNT, BNNT@MS and BNNT@MS–NH_2 samples, as shown in Fig. 2B. BNNTs showed a typical adsorption spectrum of B–N stretching vibration at 1372 cm^{-1} and B–N–B bending vibration at 800 cm^{-1}.[15] For BNNT@MS, the adsorption band at 1080 cm^{-1} corresponding to Si–O–Si groups appeared.[16] BNNT@MS–NH_2 revealed new shoulder bands at around 1600 cm^{-1} associated with the asymmetric and symmetric bending of amino groups (–NH_2)[17] and obscure bands at 1080 cm^{-1} associated with Si–O–Si vibration. The amount of amino group was determined to be (2.5 ± 1.2) × 10^{-4} mol g^{-1}.

The chemotherapy drug dox was then loaded onto BNNTs and BNNTs functionalized with mesoporous silica to check the drug loading ability. The pH-dependent dox loading on BNNTs was observed, as illustrated in Fig. S4A (ESI†). Similar pH-dependent loading of dox was found for BNNT@MS and BNNT@MS–NH_2 (data not shown). The loading efficiency of dox on BNNTs increased with an increase in the pH value. The pK_a of dox is 8.2. Dox is considered hydrophilic at lower pH because of the presence of the positively charged amino –NH_3^+ group. The increased deprotonation of –NH_2 groups on dox at a higher pH = 9.0 accounts for the increased hydrophobicity and decreased solubility of dox,[18] which results in the increase in the interaction between dox and BNNTs. TEM images revealed the presence of amorphous substances on BNNTs, which provides the evidence for the loading of dox on them (Fig. S5, ESI†). When doxorubicin was loaded at a pH of about 9.0, BNNTs, BNNT@MS and BNNT@MS–NH_2 showed almost the same doxorubicin loading amounts (Fig. S4B, ESI†). BNNTs and functionalized BNNTs allow π-stacking of dox with an ultrahigh loading capacity of ~60% by weight at a pH value of 9.0. It should be pointed out here that the hydrophobic nature of BNNTs facilitated the loading of dox at such high pH. And the presence of interconnected mesopores in BNNT@MS and BNNT@MS–NH_2 provides the route for the diffusion of dox and loading on the uncovered surface of BNNTs.

To investigate the cellular internalization of dox loaded on different BNNT samples, *i.e.* those functionalized with mesoporous silica, the dox loaded BNNT samples were added to LNcap prostate cancer cells and incubated for 5 h at 37 °C (Fig. 3A and Fig. S6, ESI†). For BNNTs, BNNT@MS or BNNT@MS–NH_2, the loading of dox onto them significantly enhanced the amounts of internalized dox uptaken by LNcap prostate cancer cells, about 3–4 times compared with a free dox. The enhanced internalization of dox through loading onto nanotubes is thought to be due to the different uptake mechanisms, as the dox-loaded particles are internalized by the endocytosis process,[19] compared with a free dox, which enters cells by passive diffusion.[20] As for BNNTs, BNNT@MS

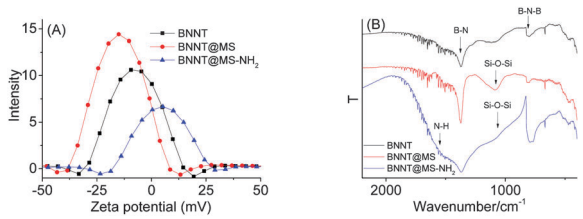

Fig. 2 (A) Zeta potential and (B) FTIR spectra of BNNT, BNNT@MS and BNNT@MS–NH_2 samples.

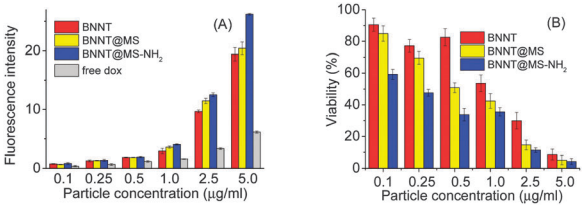

Fig. 3 (A) Fluorescence intensity of intracellular uptake of dox by LNcap prostate cancer cells for BNNT, BNNT@MS and BNNT@MS–NH_2 samples loaded with dox and medium with corresponding amount of free dox after being cultured at 37 °C for 5 h; (B) viability of LNcap prostate cancer cells after culturing with a medium containing different amounts of BNNT, BNNT@MS and BNNT@MS–NH_2 loaded with dox at 37 °C for 24 h.

or BNNT@MS–NH_2 samples, the amounts of the internalized dox were BNNT concentration-dependent. With the increase in nanotube concentration, the internalized dox amounts increased. BNNT@MS and BNNT@MS–NH_2 hybrids showed higher dox intracellular delivery ability than BNNTs. BNNTs functionalized with mesoporous silica exhibited increased suspension ability, which may account for increased dox internalization. Generally, the uptake efficiency depends on the particle size, zeta potential and so on. Particles with a small size and good suspension ability exhibit higher uptake efficiency than those with a large size and poor suspension ability.[21] Particles with a neutral surface possess the lowest uptake efficiency, while particles with a positive charge reveal higher uptake efficiency than those with a negative charge.[22] Functionalization of BNNTs with mesoporous silica improved their suspension ability, which resulted in a higher uptake of dox-loaded particles by cancer cells. In addition, BNNT@MS–NH_2 samples displayed higher dox intracellular delivery ability than BNNT@MS ones, because the zeta potential of cell membranes is normally negative ranging from −40 to −80 mV, and more positively charged particles generally displayed higher uptake by cells.[22] Thus through the adjustment of the surface functional groups on BNNTs, the cellular uptake properties of the loaded drug molecules were effectively manipulated.

To further examine whether the surface functionalization of BNNTs with mesoporous silica can effectively influence the chemotherapy efficacy of dox, the dox loaded BNNTs, and BNNT@MS and BNNT@MS–NH_2 hybrids were cocultured with LNcap prostate cancer cells to check their cancer cell killing ability. As shown in Fig. 3B, BNNTs, BNNT@MS or BNNT@MS–NH_2 samples with dox all showed cancer cell killing ability in a concentration-dependent manner. The cancer cell killing ability follows the sequence: BNNT@MS–NH_2 > BNNT@MS > BNNTs, which is in accordance with the amounts of internalized dox. As mentioned above, the increased suspension ability and hydrophilic properties, and the increased dox internalization by cancer cells were obtained when BNNTs were functionalized with mesoporous silica, which resulted in increased cancer cell killing ability. Similarly, positively charged BNNT@MS–NH_2 exhibited higher cancer cell killing ability than negatively charged BNNT@MS due to the increased dox uptake by cancer cells.

In conclusion, BNNT@mesoporous silica composites with a negative charge and a positive charge were fabricated for intracellular delivery of chemotherapy drug dox into LNcap prostate cancer cells. The loading of dox onto functionalized BNNTs increased the endocytosis efficiency of dox 3–4 times compared with free dox. BNNTs functionalized with mesoporous silica showed increased suspension ability and hydrophilic properties, increased dox internalization by cancer cells and increased cancer cell killing ability. Positively charged BNNT@MS–NH_2 samples displayed higher dox internalization and cancer cell killing ability than negatively charged BNNT@MS samples. These results provide exciting opportunities for the functionalization of BNNT vehicles in biomedical applications, especially in cancer therapy.

Notes and references

1 D. Lahiri, F. Rouzaud, T. Richard, A. K. Keshri, S. R. Bakshi, L. Kos and A. Agarwal, *Acta Biomater.*, 2010, **6**, 3524–3533; D. Lahiri, V. Singh, A. P. Benaduce, S. Seal, L. Kos and A. Agarwal, *J. Mech. Behav. Biomed. Mater.*, 2011, **4**, 44–56.
2 G. Ciofani, V. Raffa, J. Yu, Y. Chen, Y. Obata, S. Takeoka, A. Menciassi and A. Cuschieri, *Curr. Nanosci.*, 2009, **5**, 33–38.
3 D. A. Buzatu, J. G. Wilkes, D. Miller, J. A. Darsey, T. Heinze, A. Biris, R. Berger and M. Diggs, *US Pat.*, 7608240, 2009.
4 V. Raffa, C. Riggio, M. W. Smith, K. C. Jordan, W. Cao and A. Cuschieri, *Technol. Cancer Res. Treat.*, 2012, **11**, 459–465.
5 X. Chen, P. Wu, M. Rousseas, D. Okawa, Z. Gartner, A. Zettl and C. R. Bertozzi, *J. Am. Chem. Soc.*, 2009, **131**, 890–891; G. Ciofani, S. Danti, D. D'Alessandro, L. Ricotti, S. Moscato, G. Bertoni, A. Falqui, S. Berrettini, M. Petrini, V. Mattoli and A. Menciassi, *ACS Nano*, 2010, **4**, 6267–6277.
6 L. Horvath, A. Magrez, D. Golberg, C. Y. Zhi, Y. Bando, R. Smajda, E. Horvath, L. Forro and B. Schwaller, *ACS Nano*, 2011, **5**, 3800–3810.
7 Z. Yinghuai, A. T. Peng, K. Carpenter, J. A. Maguire, N. S. Hosmane and M. Takagaki, *J. Am. Chem. Soc.*, 2005, **127**, 9875–9880.
8 T. A. Hilder and J. M. Hill, *Micro Nano Lett.*, 2008, **3**, 18–24.
9 C. Y. Zhi, Y. Bando, C. C. Tang, R. G. Xie, T. Sekiguchi and D. Golberg, *J. Am. Chem. Soc.*, 2005, **127**, 15996–15997.
10 Z. H. Gao, C. Y. Zhi, Y. Bando, D. Golberg and T. Serizawa, *J. Am. Chem. Soc.*, 2010, **132**, 4976–4977.
11 C. Y. Zhi, N. Hanagata, Y. Bando and D. Golberg, *Chem.–Asian. J.*, 2011, **6**, 2530–2535.
12 N. Prabhakar, T. Nareoja, E. von Haartman, D. Sen Karaman, H. Jiang, S. Koho, T. A. Dolenko, P. E. Hanninen, D. I. Vlasov, V. G. Ralchenko, S. Hosomi, I. I. Vlasov, C. Sahlgren and J. M. Rosenholm, *Nanoscale*, 2013, **5**, 3713–3722.
13 X. Lu, H. Liu, C. Deng and X. Yan, *Chem. Commun.*, 2011, **47**, 1210–1212.
14 C. Tang, Y. Bando, T. Sato and K. Kurashima, *Chem. Commun.*, 2002, 1290–1291; C. Y. Zhi, Y. Bando, C. C. Tan and D. Golberg, *Solid State Commun.*, 2005, **135**, 67–70.
15 A. Pakdel, X. B. Wang, C. Y. Zhi, Y. Bando, K. Watanabe, T. Sekiguchi, T. Nakayama and D. Golberg, *J. Mater. Chem.*, 2012, **22**, 4818–4824.
16 X. P. Wang, X. Li, A. Ito and Y. Sogo, *Acta Biomater.*, 2011, **7**, 3638–3644.
17 Q. M. Ji, T. Yamazaki, N. Hanagata, M. V. Lee, J. P. Hill and K. Ariga, *Chem. Commun.*, 2012, **48**, 8496–8498.
18 Z. Liu, X. M. Sun, N. Nakayama-Ratchford and H. J. Dai, *ACS Nano*, 2007, **1**, 50–56.
19 L. Bildstein, C. Dubernet and P. Couvreur, *Adv. Drug Delivery Rev.*, 2011, **63**, 3–23.
20 T. Skovsgaard and N. I. Nissen, *Pharmacol. Ther.*, 1982, **18**, 293–311; G. Speelmans, R. W. H. M. Staffhorst, B. de Kruijff and F. A. de Wolf, *Biochemistry*, 1994, **33**, 13761–13768.
21 M. Motskin, D. M. Wright, K. Muller, N. Kyle, T. G. Gard, A. E. Porter and J. N. Skepper, *Biomaterials*, 2009, **30**, 3307–3317.
22 S. E. A. Gratton, P. A. Ropp, P. D. Pohlhaus, J. C. Luft, V. J. Madden, M. E. Napier and J. M. DeSimone, *Proc. Natl. Acad. Sci. U. S. A.*, 2008, **105**, 11613–11618.